

Influence of calcination temperature on structure and dielectric properties of $\text{Ca}_{0.8}\text{Sm}_{0.4/3}\text{TiO}_3$ ceramics prepared via solid-state reaction

Chun-Hsu Shen*

Department of Electronic Engineering, Ming Chuan University, 5 De Ming Rd., Gui Shan District, Taoyuan City 333, Taiwan, ROC

Received 19 May 2025; received in revised form 14 June 2025; accepted 20 June 2025

Abstract

This study investigates the effect of calcination and sintering conditions on structure and dielectric properties of $\text{Ca}_{0.8}\text{Sm}_{0.4/3}\text{TiO}_3$ ceramics synthesized via solid-state reaction. The powders calcined at temperatures ranging from 1000 to 1200 °C were sintered at temperatures between 1375 and 1500 °C for various holding times (1–5 h). X-ray diffraction analyses confirmed single-phase perovskite formation, revealing optimal crystallinity and high phase purity at a calcination temperature of 1100 °C and sintering temperature of 1425 °C for 4 h. Scanning electron microscopy showed significant grain growth and reduced porosity at higher sintering temperatures and optimal holding times. Energy-dispersive spectroscopy indicated homogeneous elemental distribution. Dielectric measurements demonstrated that optimized sintering conditions enhanced permittivity and quality factors ($Qf \sim 14900$ GHz), as well as improved frequency stability ($\tau_f \sim 387$ ppm/°C). Furthermore, the composite ceramics formed with $\text{Mg}_{0.95}\text{Co}_{0.05}\text{TiO}_3$ significantly improved dielectric properties and frequency stability, making these materials promising for advanced microwave device applications.

Keywords: $\text{Ca}_{0.8}\text{Sm}_{0.4/3}\text{TiO}_3$, calcination and sintering conditions, structure, microwave dielectric properties

I. Introduction

Microwave dielectric ceramics have attracted significant attention recently due to their critical roles in modern communication devices, such as resonators, filters and antennas [1–8]. The rapid development of communication technology, particularly in high-frequency and miniaturized systems, demands materials with superior dielectric properties, including high dielectric constant, low dielectric loss and stable frequency characteristics under various environmental conditions. Advanced dielectric ceramics, particularly perovskite-type titanates such as CaTiO_3 , exhibit excellent intrinsic dielectric properties, but their performance is frequently limited by temperature-dependent dielectric instability and relatively high dielectric loss. To address these limitations, the performance of dielectric ceramics can be significantly enhanced through strategic doping with rare-earth elements and precise optimization of processing conditions [9–12].

The incorporation of rare-earth elements, particularly Sm^{3+} , into CaTiO_3 ceramics has garnered extensive research interest due to its potential to tailor dielectric properties, improve microstructural uniformity and enhance temperature stability. Sm^{3+} ions, with their unique ionic radii and valence states, contribute to lattice distortion and modify structural properties, thereby influencing phase stability, grain growth and ultimately dielectric performance [9]. Processing parameters, especially calcination and sintering conditions, critically influence phase purity, microstructural development and dielectric behaviour. Optimized calcination conditions ensure complete solid-state reactions, eliminate residual phases and produce uniformly reactive powders. Sintering parameters facilitate densification, promote grain growth and reduce porosity, thereby significantly enhancing dielectric properties [13–21].

Despite significant research efforts, systematic studies, especially those investigating the combined effects of calcination temperature and sintering parameters on the structural and dielectric properties of Sm-doped CaTiO_3 ceramics, remain limited. Thus, this study specifically focuses on the synthesis and

*Corresponding author: tel: +886 3 350 7001 ext. 3737
e-mail: chshen0656@mail.mcu.edu.tw

optimization of $\text{Ca}_{0.8}\text{Sm}_{0.4/3}\text{TiO}_3$ ceramics, evaluating how calcination temperature and sintering conditions impact ceramics' structure and microwave dielectric properties. Recent studies have increasingly explored rare-earth element doping, composite strategies and multi-site substitution in perovskite ceramics to simultaneously improve dielectric constant, Qf and τ_f [13,19–22]. These developments provide important context for the design of thermally stable and high-performance microwave ceramics. This research aims to provide valuable insights into the optimization of processing conditions for enhanced dielectric performance, supporting the practical application of $\text{Ca}_{0.8}\text{Sm}_{0.4/3}\text{TiO}_3$ ceramics in high-performance microwave devices through comprehensive structural characterization and dielectric measurement.

II. Experimental

Ceramic powders of $\text{Ca}_{0.8}\text{Sm}_{0.4/3}\text{TiO}_3$ were synthesized via the conventional solid-state reaction route. High-purity analytical-grade CaCO_3 (99%, Showa), Sm_2O_3 (99.9%, Showa) and TiO_2 (99%, Acros) powders were used as starting materials. These powders were accurately weighed according to the stoichiometric proportions and thoroughly mixed through ball milling in ethanol using zirconia media for 24 h to ensure compositional uniformity and particle size homogeneity. The resulting slurry was subsequently dried in an oven at 150 °C, and the dried powder was ground to break up agglomerates.

To investigate the influence of calcination temperature on phase formation and microstructural evolution, the mixed powders were calcined at various temperatures ranging from 1000 to 1200 °C with holding times of 1–6 h in air. After calcination, the powders were pulverized and sieved through a 100-mesh screen and mixed with a small amount of polyvinyl alcohol (PVA) binder solution (approximately 3 wt.%). The powders were pressed into cylindrical pellets with dimensions of roughly 11 mm in diameter and 5 mm thick at a pressure of ~2000 MPa.

The green pellets were then sintered at temperatures between 1350 and 1500 °C for 1–5 h under ambient atmosphere, with heating and cooling rates fixed at 10 °C/min. After sintering, the pellets were polished for microstructural analyses. Relative density (ρ_r) was determined to evaluate the densification of the sintered ceramics. It is defined as the ratio of the measured bulk density (ρ_{bulk}) to the theoretical density (ρ_{th}) of the material. The bulk density was measured using the Archimedes method in deionized water. The relative density was calculated according to the following equation:

$$\rho_r = \frac{\rho_{bulk}}{\rho_{th}} \times 100 \quad (1)$$

The theoretical density ρ_{th} was calculated using lattice parameters obtained from XRD analysis and the known molecular weight and unit cell volume of $\text{Ca}_{0.8}\text{Sm}_{0.4/3}\text{TiO}_3$. The open porosity (P) was then estimated using the relation:

$$P = \left(1 - \frac{\rho_{bulk}}{\rho_{th}} \right) \times 100 \quad (2)$$

Phase identification and crystal structure characterization were performed using X-ray diffraction (XRD, Siemens D5000, Munich, Germany, Cu-K α radiation, $\lambda = 1.5406 \text{ \AA}$) over the 2θ range from 20° to 80° with a scan step of 0.02° and a scan rate of 2 °/min. Microstructural features, including grain morphology and grain size distribution, were examined using scanning electron microscopy (SEM, Philips XL-40FEG, Eindhoven, the Netherlands) with energy-dispersive X-ray spectroscopy (EDS) for elemental analysis.

For dielectric properties measurements, silver electrodes were applied to both surfaces of the polished ceramic pellets by screen-printing, followed by heat treatment at 600 °C for 30 min to enhance electrode adhesion. Dielectric properties, including dielectric constant (ϵ_r), quality factor (Qf) and temperature coefficient of resonant frequency (τ_f), were measured near 8 GHz using the Hakki-Coleman dielectric resonator method [22–24]. The measured frequency corresponds to the fundamental $TE_{01\delta}$ resonant mode of the sample, which varies slightly depending on sample geometry and dielectric constant. Since the Hakki-Coleman method is a resonance-based technique, dielectric properties are typically reported at this dominant microwave frequency and frequency-swept measurements are not employed.

In addition, composite samples containing $\text{Ca}_{0.8}\text{Sm}_{0.4/3}\text{TiO}_3$ phase were also prepared. Thus, the composite $(1-x)\text{Mg}_{0.95}\text{Co}_{0.05}\text{TiO}_3-x\text{Ca}_{0.8}\text{Sm}_{0.4/3}\text{TiO}_3$ powders, where $x = 0.05, 0.10, 0.15$ and 0.20 , were obtained by mixing of two calcined powders, and after that uniaxially pressed and sintered at 1225–1325 °C for 4 h.

III. Results and discussion

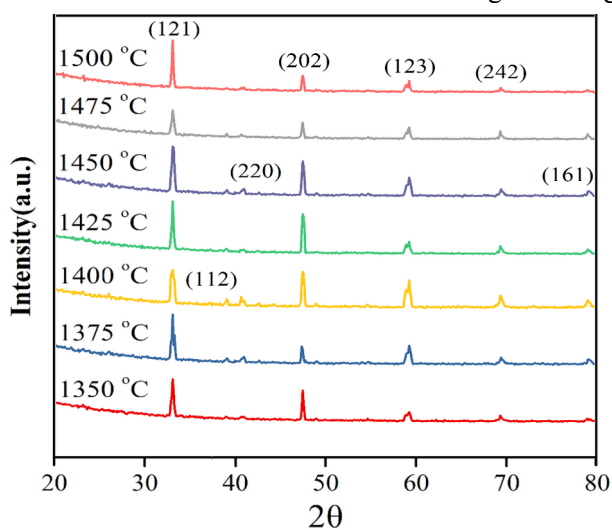
3.1. Structural characterization

To better understand the impact of each processing step, XRD patterns were grouped into two categories: i) those obtained after calcination and ii) those after sintering. The former aims to evaluate the phase development and crystallinity after calcination, while the latter assesses the effects of final densification and grain growth on crystal structure. Figure 1 illustrates the XRD patterns of the precursor

powders after calcination at temperatures ranging from 1000 to 1200 °C, held for 1 to 6 h. As the calcination temperature and duration time increase a notable enhancement in peak intensities is observed, indicating improved crystallinity and more complete solid-state reactions. No significant impurity peaks were detected, confirming the successful synthesis of a single-phase perovskite structure, which matched well with the standard JCPDS card (No. 42-0423). The intensity scale is shown in Fig. 1 to highlight relative peak development under different calcination conditions and peak indexing and phase assignment are provided in Fig. 2.

Figure 2 demonstrates the influence of sintering temperature (1350–1500 °C) and holding time (1–5 h) on the phase formation and crystallinity. Distinct peaks corresponding to the primary perovskite planes, such as (112), (121), (220), (202), (123), (242) and (161), became sharper and more intense with increased sintering temperatures and extended holding times, further confirming the enhancement of crystallinity and grain growth [25]. Although increased sintering temperature and time typically enhance crystallinity, the peak intensity is not always increased monotonically. This may be due to the grain coarsening, porosity redistribution, or microstructural heterogeneity that influences diffraction coherence. Optimal phase purity and crystallinity appeared to be achieved around 1450–1500 °C after 4–5 h of sintering, as indicated by the clearly defined and intense diffraction peaks. The progressive refinement in crystallinity, as evidenced by XRD peak sharpening, combined with microstructural densification observed in SEM, contributes to enhanced dielectric performance, particularly the elevated Q_f and improved thermal stability, making the material more suitable for microwave device applications.

The lattice parameters of the $\text{Ca}_{0.8}\text{Sm}_{0.4/3}\text{TiO}_3$ ceramics under different sintering conditions are summarized in Table 1. With increasing sintering



temperature from 1375 to 1500 °C (holding time fixed at 4 h), slight fluctuations in the lattice parameters (a , b and c) were observed. Specifically, lattice parameters varied within narrow ranges (a : 5.4171–5.4465 Å, b : 7.6379–7.6609 Å, c : 5.3863–5.3885 Å), indicating minimal structural changes consistent with the stable perovskite structure under these conditions [26]. When the holding time was varied from 1 to 5 h at a fixed temperature of 1425 °C, the lattice parameters remained relatively stable after 2 h, suggesting that equilibrium in crystal growth and structural stability were achieved within this time frame. These results corroborate the XRD findings, confirming improved crystallinity and structural homogeneity with optimized sintering parameters.

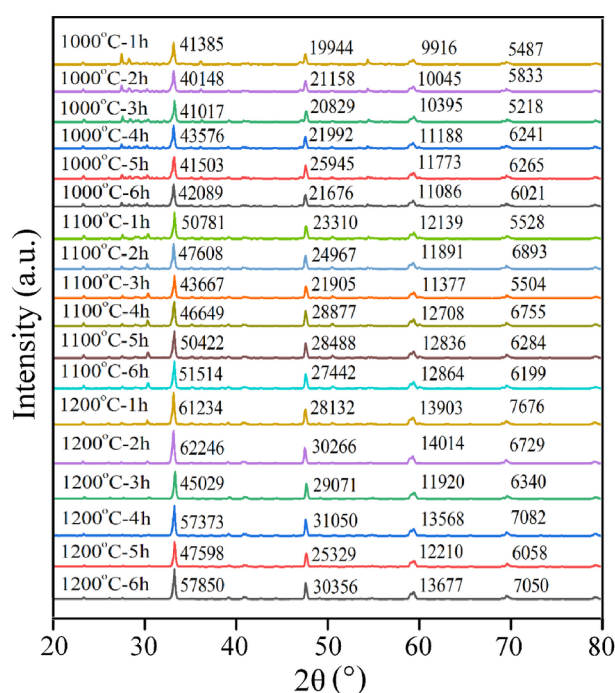


Figure 1. XRD results of $\text{Ca}_{0.8}\text{Sm}_{0.4/3}\text{TiO}_3$ ceramics at different calcination temperatures and holding times

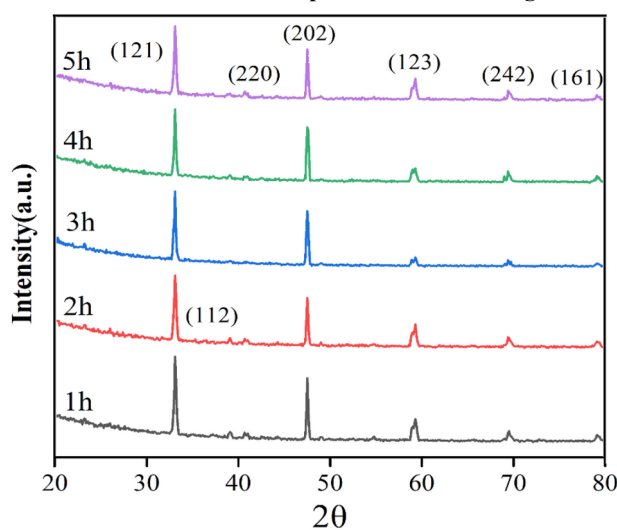


Figure 2. XRD patterns of $\text{Ca}_{0.8}\text{Sm}_{0.4/3}\text{TiO}_3$ ceramics (a) sintered at various temperatures for 4 h and (b) sintered at 1425 °C for different holding times

SEM images in Figs. 3 and 4 illustrate the microstructural evolution of the $\text{Ca}_{0.8}\text{Sm}_{0.4/3}\text{TiO}_3$ ceramics under various sintering temperatures and durations. At lower sintering temperatures (1375–1425 °C), the ceramics exhibited smaller grain sizes with

clear grain boundaries. As sintering temperatures increased to 1450 °C and beyond, significant grain growth occurred and grains became larger and more uniform, indicating enhanced densification and reduced porosity (Fig. 3). Grain size estimation based

Table 1. The lattice parameters of $\text{Ca}_{0.8}\text{Sm}_{0.4/3}\text{TiO}_3$ ceramics under various sintering conditions

Sintering temperature [°C]	Holding time [h]	a [Å]	b [Å]	c [Å]
1375	4	5.4368±0.0091	7.6597±0.0061	5.3876±0.0056
1400	4	5.4171±0.0158	7.6609±0.0171	5.3867±0.0156
1425	4	5.4465±0.0046	7.6586±0.0049	5.3885±0.0045
1450	4	5.4352±0.0049	7.6379±0.0052	5.3863±0.0048
1475	4	5.4465±0.0046	7.6586±0.0049	5.3885±0.0045
1500	4	5.4352±0.0049	7.6379±0.0052	5.3863±0.0048
1425	1	5.4059±0.0154	7.6402±0.0166	5.3845±0.0153
1425	2	5.4465±0.0046	7.6586±0.0049	5.3885±0.0045
1425	3	5.4465±0.0046	7.6586±0.0049	5.3885±0.0045
1425	4	5.4465±0.0046	7.6586±0.0049	5.3885±0.0045
1425	5	5.4465±0.0046	7.6586±0.0049	5.3885±0.0045

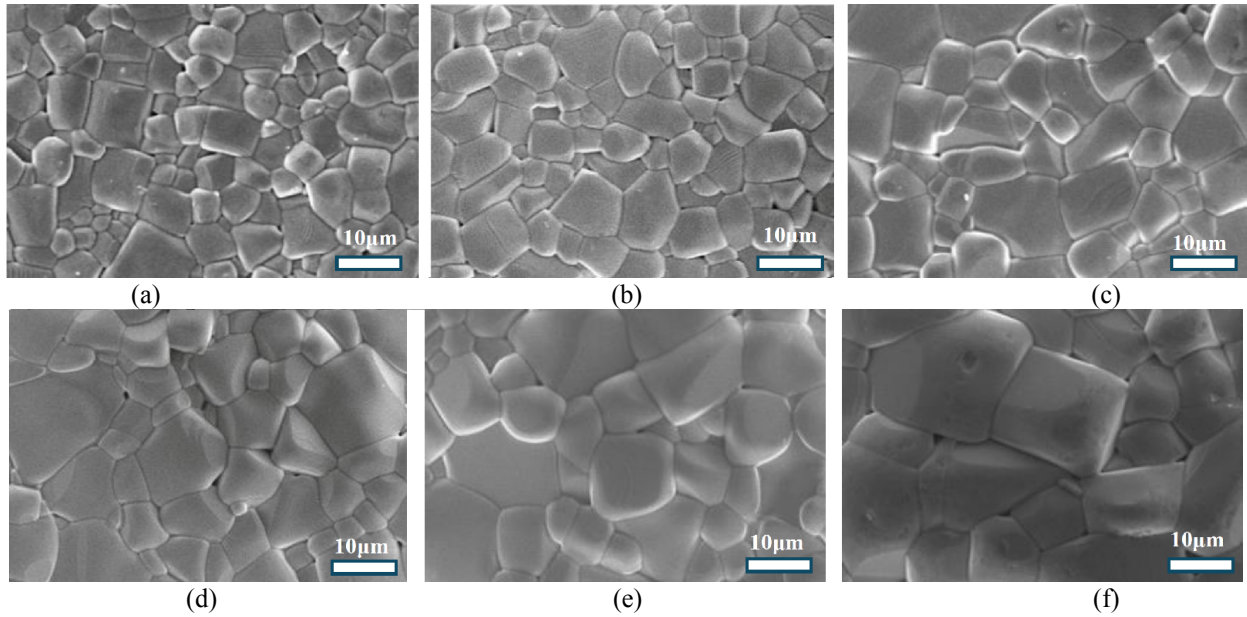


Figure 3. Microstructural evolution of $\text{Ca}_{0.8}\text{Sm}_{0.4/3}\text{TiO}_3$ ceramics observed via SEM at various sintering temperatures: a) 1375 °C, b) 1400 °C, c) 1425 °C, d) 1450 °C, e) 1475 °C and f) 1500 °C for 4 h

on SEM images indicates that the average grain size increases from ~1.5 μm at 1375 °C to ~3.5 μm at 1500 °C (4 h), consistent with thermally driven grain coarsening and enhanced densification behaviour. The variation observed in the XRD pattern of the 1475 °C sample is likely due to the increased grain size and surface roughness, which can reduce diffraction coherence and alter background intensity. All XRD measurements were performed under identical instrumental conditions, confirming that the differences arise from microstructural effects rather than measurement inconsistencies. Extended sintering durations at 1425 °C resulted in grain growth and improved microstructural uniformity as shown by

SEM images (Fig. 4). Meanwhile, XRD patterns showed peak sharpening, indicative of enhanced crystallinity. These two observations together support the conclusion that prolonged sintering improves both structural and microstructural quality of the ceramics. These SEM observations support the findings from the lattice parameter analysis and suggest that controlled sintering conditions effectively enhance the microstructural characteristics, contributing positively to the material's dielectric performance [27,28]. Although quantitative grain size measurements were not performed, SEM observations revealed clear trends of grain coarsening and densification with increasing

sintering temperature, which are consistent with the improvements observed in dielectric properties.

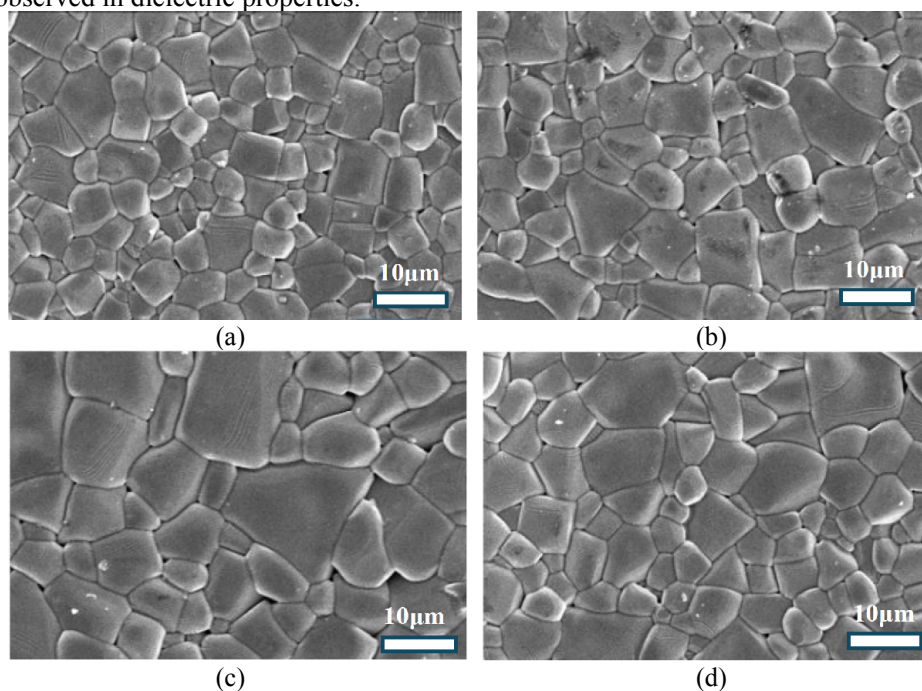


Figure 4. SEM micrographs of $\text{Ca}_{0.8}\text{Sm}_{0.4/3}\text{TiO}_3$ ceramics sintered at 1425 °C for various times: a) 1 h, b) 2 h, c) 3 h and d) 4 h

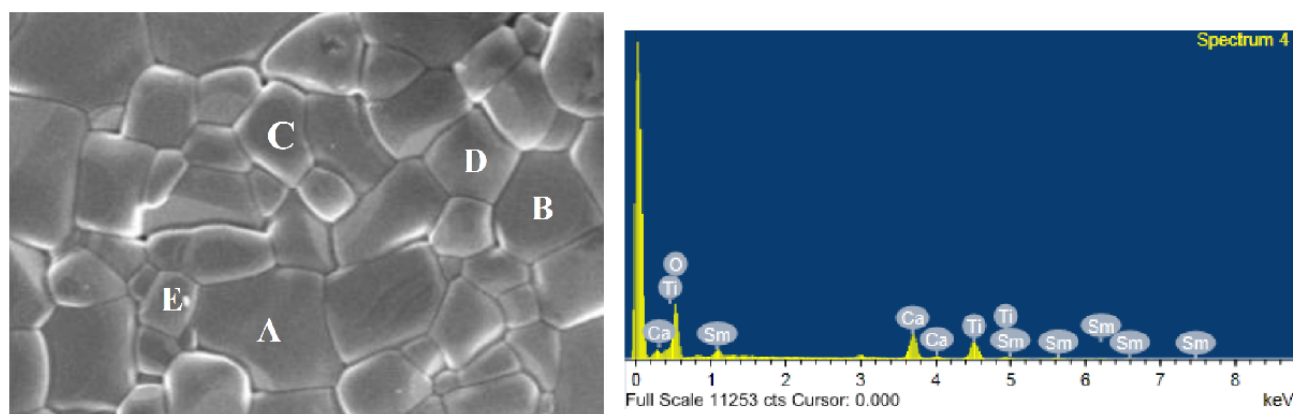


Figure 5. EDS results of $\text{Ca}_{0.8}\text{Sm}_{0.4/3}\text{TiO}_3$ ceramics sintered at 1425 °C, including full-area elemental mapping and spot analyses on selected grains in Table 2

Table 2. EDS results of for various spots in Fig. 5

Spot	Composition [at.%]			
	Ca	Sm	Ti	O
A	10.95	2.3	12.08	74.67
B	8.79	1.85	9.71	79.65
C	8.06	1.69	8.89	81.36
D	7.98	1.67	8.81	81.54
E	6.62	1.39	7.31	84.68

Energy-dispersive spectroscopy (EDS) results shown in Fig. 5 and Table 2 confirm the elemental composition of the $\text{Ca}_{0.8}\text{Sm}_{0.4/3}\text{TiO}_3$ ceramics. The EDS analyses reveal the presence of calcium Ca, Sm, Ti and O, and the atomic ratios of Ca, Sm and Ti were consistent with the nominal stoichiometry across all measured points. The observed variations were mainly

due to fluctuations in the oxygen content, likely caused by the limited sensitivity of EDS in detecting light elements. Nonetheless, these compositional variations remained minimal, supporting the homogeneous distribution of constituent elements and confirming the formation of a consistent perovskite structure. These structural and compositional improvements, evidenced

by XRD and EDS analyses, are expected to positively influence dielectric performance, as confirmed by the measured ϵ_r and Qf values presented in the following sections.

The relative density and porosity of the $\text{Ca}_{0.8}\text{Sm}_{0.4/3}\text{TiO}_3$ ceramics as a function of sintering temperature and holding time are presented in Fig. 6. As the sintering temperature increased to around 1425

$^{\circ}\text{C}$, the relative density reached a maximum, while porosity reached a minimum, indicating optimal densification. Beyond this temperature, a slight decrease in density and increased porosity were observed, likely due to the grain coarsening and possible microstructural defects at higher temperatures [29].

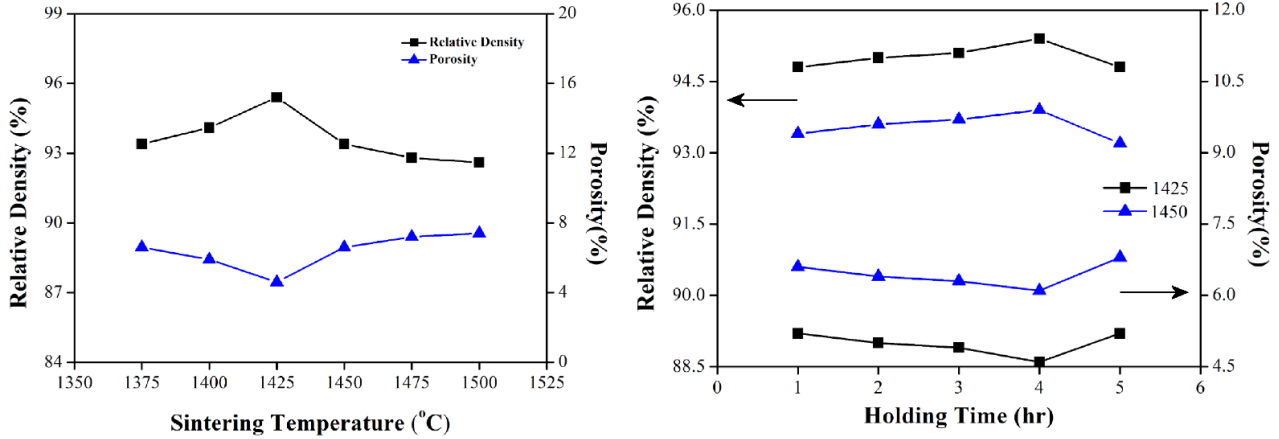


Figure 6. Relative density and porosity of $\text{Ca}_{0.8}\text{Sm}_{0.4/3}\text{TiO}_3$ ceramics as a function of holding time and sintering temperature

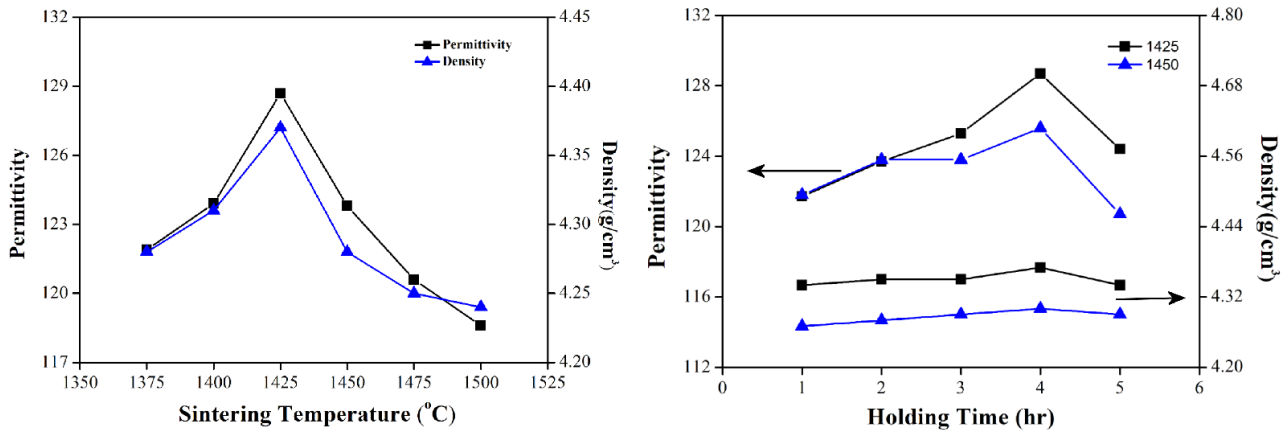


Figure 7. Dielectric constant (ϵ_r) of $\text{Ca}_{0.8}\text{Sm}_{0.4/3}\text{TiO}_3$ ceramics as a function of sintering conditions, measured at ~ 8 GHz

3.2. Dielectric properties

The dielectric constant (ϵ_r) of the $\text{Ca}_{0.8}\text{Sm}_{0.4/3}\text{TiO}_3$ ceramics as a function of sintering temperature and holding time are presented in Fig. 7. The change of ϵ_r has similar trend as that for density. Thus, the dielectric constant (ϵ_r) peaked at approximately 1425 $^{\circ}\text{C}$, correlating closely with the density results. The improved dielectric properties are directly associated with the enhanced densification, reduced porosity and homogeneous microstructure observed in SEM images and confirmed by XRD and EDS analyses. These correlations highlight the importance of controlling sintering conditions to achieve ceramics with superior structure and dielectric performances.

The quality factor (Qf) and the temperature coefficient of resonant frequency (τ_f) for the

$\text{Ca}_{0.8}\text{Sm}_{0.4/3}\text{TiO}_3$ ceramics are illustrated in Fig. 8. The Qf value increased significantly with the rise in sintering temperature up to the maximum of ~ 14900 GHz at 1425 $^{\circ}\text{C}/4$ h, but starts to decline at higher temperatures. This is consistent with the optimal microstructural features, such as well-packed grains and minimal porosity, observed via SEM. The corresponding dielectric loss ($\tan \delta$) was calculated using the relation $\tan \delta = f / Qf$, with $f \approx 8$ GHz. The increase in Qf with sintering temperature is attributed to the improved densification and microstructural homogeneity, which reduce extrinsic dielectric loss mechanisms such as grain boundary scattering. No secondary phases were detected by XRD, further supporting the structural purity of the ceramics. In addition, intrinsic dielectric loss in crystals originates from lattice vibrations, ionic polarizability and phonon

interactions, and sets a fundamental limit to the maximum achievable Qf . This intrinsic loss can be minimized by forming a highly ordered and chemically homogeneous lattice, achieved through optimized sintering and precise stoichiometry [30,31]. However, the τ_f values exhibited minor variation with sintering temperature or holding time. This behaviour indicates that τ_f is primarily governed by the intrinsic characteristics of the material's crystal structure and ionic configuration, especially the nature of the A-site cation substitution with Sm^{3+} for Ca^{2+} , which strongly

influences the dielectric polarization mechanisms and thermal response of the resonant frequency. The results reinforce that while Qf can be enhanced by tailoring sintering parameters and improving microstructure, τ_f is primarily dictated by compositional design and intrinsic lattice dynamics. To further examine the influence of calcination temperature under constant sintering conditions, Table 3 summarizes the dielectric properties of the $\text{Ca}_{0.8}\text{Sm}_{0.4/3}\text{TiO}_3$ ceramics calcined at 1100 and 1200 °C, both sintered at 1425 °C for 4 h.

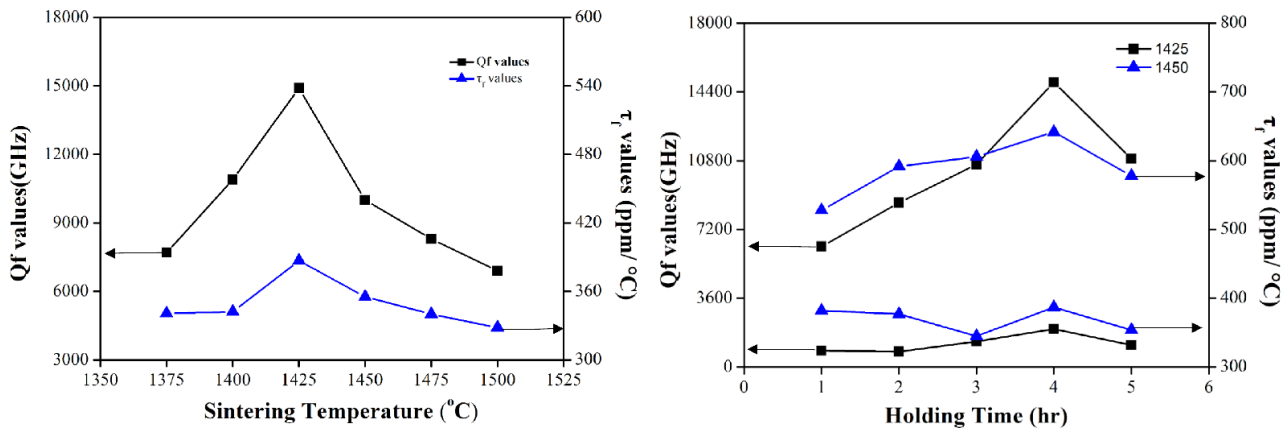


Figure 8. Qf and τ_f values of $\text{Ca}_{0.8}\text{Sm}_{0.4/3}\text{TiO}_3$ ceramics sintered at different temperatures (a) and holding times (b)

Table 3. Dielectric properties of $\text{Ca}_{0.8}\text{Sm}_{0.4/3}\text{TiO}_3$ ceramics calcined at different temperatures (1100 and 1200 °C), both sintered at 1425 °C for 4 h

	Calcination conditions	ϵ_r	Qf [GHZ]	τ_f [ppm/°C]
[9]	1100 °C/4h	120	13,000	+400
This work	1200 °C/2h	128.7	14,900	+386.9
Comparison		+7.25%	+14.62%	-3.3%

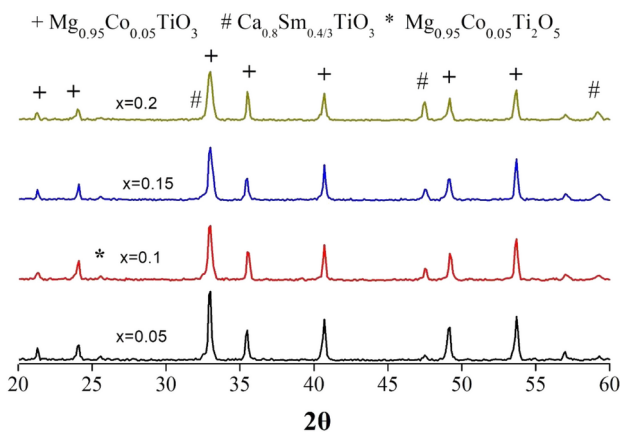


Figure 9. XRD patterns of $(1-x)\text{Mg}_{0.95}\text{Co}_{0.05}\text{TiO}_3 - x\text{Ca}_{0.8}\text{Sm}_{0.4/3}\text{TiO}_3$ ceramics with various x values, sintered at their respective optimal temperatures for 4 h

In summary, the results demonstrate that optimization of the sintering temperature and holding time significantly improves crystallinity, densification and microstructural uniformity, enhancing dielectric performance. Notably, the Qf values are highly

sensitive to microstructural quality and dielectric loss, while τ_f is more dependent on intrinsic material composition. These insights provide a solid foundation for further compositional engineering and processing optimization of $\text{Ca}_{0.8}\text{Sm}_{0.4/3}\text{TiO}_3$ -based ceramics for advanced microwave applications. However, the τ_f values exhibited minor variation with sintering temperature or holding time. This behaviour indicates that τ_f is primarily governed by the intrinsic characteristics of the material's crystal structure and ionic configuration, especially the nature of the A-site cation substitution with Sm^{3+} for Ca^{2+} , which strongly influences the dielectric polarization mechanisms and thermal response of the resonant frequency. The results reinforce that while Qf can be enhanced by tailoring sintering parameters and improving microstructure, τ_f is primarily dictated by compositional design and intrinsic lattice dynamics.

3.3. $\text{Mg}_{0.95}\text{Co}_{0.05}\text{TiO}_3 - \text{Ca}_{0.8}\text{Sm}_{0.4/3}\text{TiO}_3$ composite

To further improve the dielectric properties of $\text{Ca}_{0.8}\text{Sm}_{0.4/3}\text{TiO}_3$ ceramics, composite samples with molar ratios of $x = 0.05, 0.10, 0.15$ and 0.20 in the $(1-x)\text{Mg}_{0.95}\text{Co}_{0.05}\text{TiO}_3-x\text{Ca}_{0.8}\text{Sm}_{0.4/3}\text{TiO}_3$ system were prepared. Figure 9 shows the XRD patterns of $(1-x)\text{Mg}_{0.95}\text{Co}_{0.05}\text{TiO}_3-x\text{Ca}_{0.8}\text{Sm}_{0.4/3}\text{TiO}_3$ composites ($x = 0.10$ and 0.15). The diffraction peaks correspond to a combination of $\text{Mg}_{0.95}\text{Co}_{0.05}\text{TiO}_3$ and $\text{Ca}_{0.8}\text{Sm}_{0.4/3}\text{TiO}_3$ phases, with no secondary phases observed, indicating good phase compatibility between the two components.

To further verify the dielectric performance of the $(1-x)\text{Mg}_{0.95}\text{Co}_{0.05}\text{TiO}_3-x\text{Ca}_{0.8}\text{Sm}_{0.4/3}\text{TiO}_3$ composite ceramics prepared by optimized processing conditions, a composite systems with different content of $\text{Ca}_{0.8}\text{Sm}_{0.4/3}\text{TiO}_3$ phase were investigated (Fig. 10, Table 4). As the sintering temperature increased, apparent density and dielectric constant consistently improved, with the maximum near $1275\text{--}1300\text{ }^\circ\text{C}$. Notably, the Qf values were significantly enhanced for

$x = 0.10$, reaching over 120000 GHz . At the same time, the τ_f values were also tuned closer to near-zero values for higher x content, confirming that the $\text{Ca}_{0.8}\text{Sm}_{0.4/3}\text{TiO}_3$ phase effectively adjusts the thermal stability of the composite. The adjustment of τ_f values in the $(1-x)\text{Mg}_{0.95}\text{Co}_{0.05}\text{TiO}_3-x\text{Ca}_{0.8}\text{Sm}_{0.4/3}\text{TiO}_3$ composites is mainly attributed to the compositional averaging of the negative τ_f of $\text{Mg}_{0.95}\text{Co}_{0.05}\text{TiO}_3$ and the positive τ_f of $\text{Ca}_{0.8}\text{Sm}_{0.4/3}\text{TiO}_3$. No secondary phases or evident interfacial strain were detected in XRD, suggesting that the observed τ_f tuning is not dominated by lattice mismatch or phase boundary effects. These findings demonstrate that combining the well-sintered, high- ϵ_r $\text{Ca}_{0.8}\text{Sm}_{0.4/3}\text{TiO}_3$ phase with high- Q Mg-based ceramics results in a favourable balance of microwave dielectric properties. This result supports the earlier conclusions that compositional control and sintering conditions are crucial in tailoring the dielectric performance of advanced ceramics for practical microwave applications [32].

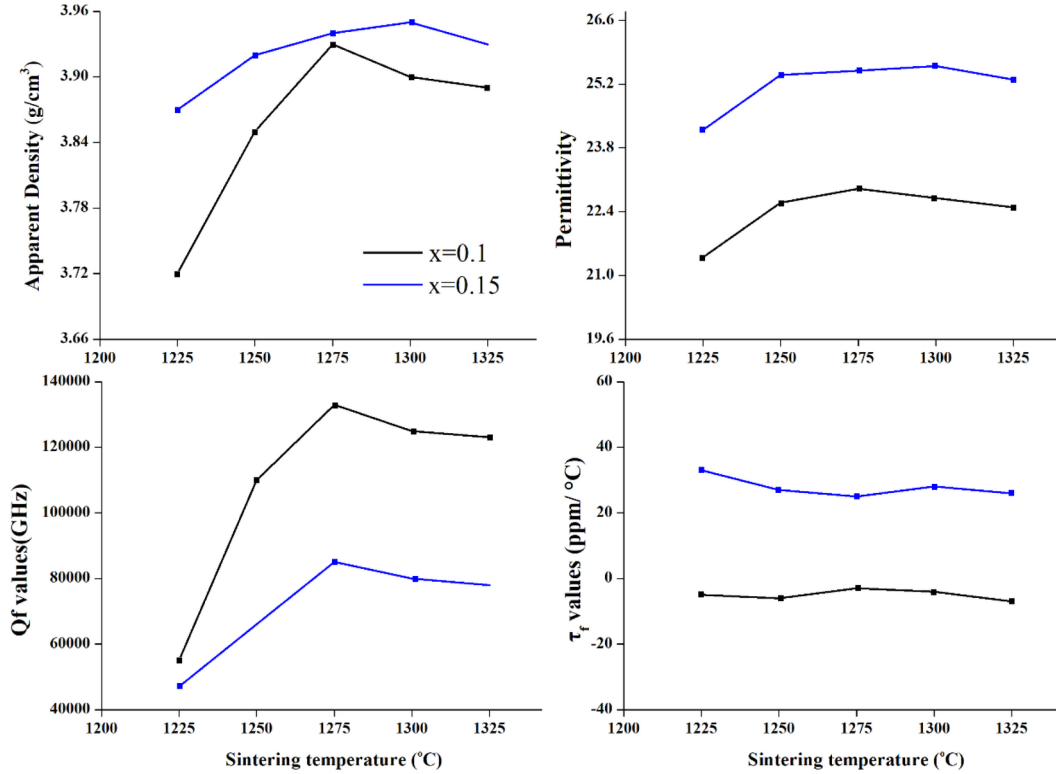


Figure 10. Variation of apparent density, dielectric constant (ϵ_r), quality factor (Qf), and temperature coefficient (τ_f) for $(1-x)\text{Mg}_{0.95}\text{Co}_{0.05}\text{TiO}_3-x\text{Ca}_{0.8}\text{Sm}_{0.4/3}\text{TiO}_3$ ceramics as a function of sintering temperature

Table 4. The dielectric performances with various x values for $(1-x)\text{Mg}_{0.95}\text{Co}_{0.05}\text{TiO}_3-x\text{Ca}_{0.8}\text{Sm}_{0.4/3}\text{TiO}_3$ ceramics

x value	Sintering temperature [$^\circ\text{C}$]	ρ [g/cm^3]	ϵ_r	Qf [GHz]	τ_f [ppm/ $^\circ\text{C}$]
0.05	1275	3.9	20.5	155,000	-30
0.10	1275	3.93	22.9	133,000	-3
0.15	1275	3.94	25.5	85,000	25
0.20	1275	3.95	28.8	70,000	54

IV. Conclusions

In this study, $\text{Ca}_{0.8}\text{Sm}_{0.4/3}\text{TiO}_3$ powder was successfully synthesized via solid-state reaction and the influence of calcination and sintering conditions on the structure and dielectric properties of the obtained ceramics was systematically investigated. XRD and SEM analyses confirmed that optimized sintering at 1425 °C for 4 h produced well-crystallized and highly densified ceramics. Dielectric measurements revealed that the highest ϵ_r and Qf values (128.7 and 14900 GHz, respectively) were achieved under these conditions, while τ_f remained relatively stable due to the compositional design. EDS analysis also confirmed chemical homogeneity, supporting structural stability. Furthermore, the integration of $\text{Ca}_{0.8}\text{Sm}_{0.4/3}\text{TiO}_3$ into $\text{Mg}_{0.95}\text{Co}_{0.05}\text{TiO}_3$ successfully enabled τ_f tuning toward near-zero values through compositional averaging, without secondary phase formation. These findings demonstrate an effective strategy for tailoring temperature stability and Qf performance through a combination of processing control and compositional design, which is essential for next-generation microwave dielectric materials.

References

- Q. Zeng, W. Li, J.L. Shi, J.K. Guo, M.W. Zuo, W.J. Wu, "A new microwave dielectric ceramic for LTCC applications", *J. Am. Ceram. Soc.*, **89** [5] (2006) 1733–1735.
- I.M. Reaney, D. Iddles, "Microwave dielectric ceramics for resonators and filters in mobile phone networks", *J. Am. Ceram. Soc.*, **89** [7] (2006) 2063–2072.
- M.T. Sebastian, H. Jantunen, "Low loss dielectric materials for LTCC applications: A review", *Int. Mater. Rev.*, **53** [2] (2008) 57–90.
- J. Bi, Y. Niu, H. Wu, "Li₄Mg₃Ti₂O₉: A novel low-loss microwave dielectric ceramic for LTCC applications", *Ceram. Int.*, **43** [10] (2017), 7522–7530.
- K. Hong, T.H. Lee, J.M. Suh, S.H. Yoon, H.W. Jang, "Perspectives and challenges in multilayer ceramic capacitors for next generation electronics", *J. Mater. Chem. C*, **7** (2019) 9782–9802.
- M.D. Hill, D.B. Cruickshank, "Perspective on ceramic materials for 5G wireless communication systems", *Appl. Phys. Lett.*, **118** (2021) 120501.
- Y. Zhang, S. Ogurtsov, V. Vasilev, A.A. Kishk, D. Caratelli, "Advanced dielectric resonator antenna technology for 5G and 6G applications", *Sensors*, **24** (2024) 1413.
- Z. Huang, J. Qiao, L. Li, "Microwave dielectric ceramics with low dielectric loss and high temperature stability for LTCC applications", *Ceram. Int.*, **50** [6] (2024) 9029–9033.
- W.S. Kim, E.S. Kim, K.H. Yoon, "Effects of Sm³⁺ substitution on dielectric properties of Ca_{1-x}Sm_{2x/3}TiO₃ ceramics at microwave frequencies", *J. Am. Ceram. Soc.*, **82** [8] (1999) 2111–2115.
- J. Kimura, H. Taniguchi, T. Iijima, T. Shimizu, S. Yasui, M. Itoh, H. Funakubo, "High temperature stability of the dielectric and insulating properties of Ca(Ti,Zr)SiO₅ ceramics", *Appl. Phys. Lett.*, **108** (2016) 062902.
- Y. Hu, "Influence of rare earth ion doping on the dielectric properties of CaTiO₃-SmAlO₃ ceramics", *Process. Appl. Ceram.*, **17** [4] (2023) 347–353.
- X. Zhang, X. Zhang, S. Ma, X. Qi, Z. Yue, "Layered-perovskite Ca_{1-x}Ba_xLa₄Ti₅O₁₇ microwave dielectric ceramics with medium dielectric constant", *Ceram. Int.*, **50** [9] (2024) 15831–15839.
- H.I. Hsiang, Y.H. Yang, C.Y. Huang, K. Yang, "Effects of calcination on the dielectric properties and insulation resistance of Ba_{0.95}Ca_{0.05}TiO₃ ceramics sintered in a reducing atmosphere", *J. Alloys Compd.*, **90** (2023) 170919.
- L.D. Vuong, N.Q. Lich, N.X. Cuong, V.Q. Nha, "Optimization of the calcination and two-step sintering temperatures of (K_{0.48}Na_{0.48}Li_{0.04})(Nb_{0.95}Sb_{0.05})O₃ ceramics", *Mater. Res. Express*, **10** (2023) 105701.
- J. Watson, G. Castro, "A review of high-temperature electronics technology and applications", *J. Mater. Sci. Mater. Electron.*, **26** (2015) 9226–9235.
- A. Zeb, S.J. Milne, "High temperature dielectric ceramics: a review of temperature-stable high-permittivity perovskites", *J. Mater. Sci. Mater. Electron.*, **26** (2015) 9243–9255.
- Q. Li, H. Du, X. Zhao, F. Zhao, Y. Zhang, X. Hu, X. Du, "Densification and microstructure evolution of NaNbO₃ ceramic via ultrafast high-temperature sintering", *Ceram. Int.*, **50** [11] (2024) 18907–18914.
- J. Li, X. Zhang, J. Liu, Q. Zhou, H. Wu, Y. Zhou, Y. Wang, W. Sun, Y. Jiang, Y. Han, Z. Han, Z. Zhao, F. Liu, W. Glaubitt, Y. Zhang, Y. Wang, L. Li, "Spinel-trirutile microwave dielectric ceramics with high Q and excellent temperature stability based on MgO-Al₂O₃-Ta₂O₅ ternary systems", *J. Eur. Ceram. Soc.*, **44** [6] (2024) 3909–3915.
- W. Guo, P. Zhao, Z. Yue, "Modification of high-temperature electrical properties in CaTiO₃ ceramics by Sm³⁺ and Al³⁺ doping", *J. Alloys Compd.* **946** (2023) 169389.
- W. Guo, Y. Yang, Z. Ma, Y. Lu, Z. Yue, "Effects of Zr⁴⁺ and Hf⁴⁺ substitution on the structure and dielectric response of Ba₄Sm_{0.933}Ti₁₈O₅₄ ceramics", *Ceram. Int.*, **50** [7] (2024) 12443–12449.
- H. Tian, X. Zhang, Z. Zhang, Y. Liu, H. Wu, "Low-permittivity LiLn(PO₃)₄ (Ln = La, Sm, Eu) dielectric ceramics for microwave/millimeter-wave communication", *J. Adv. Ceram.*, **13** [5] (2024) 602–620.
- B.W. Hakki, P.D. Coleman, "A dielectric resonator method of measuring inductive capacities in the millimeter range", *IEEE Trans. Microwave Theory Tech.*, **8** (1960) 402–410.
- S.B. Cohn, K.C. Kelly, "Microwave measurement of high dielectric constant materials", *IEEE Trans. Microwave Theory Tech.*, **14** [9] (1966) 406–410.
- W.E. Courtney, "Analysis and evaluation of a method of measuring the complex permittivity and permeability microwave insulators", *IEEE Trans. Microwave Theory Tech.*, **18** (1970) 476–485.
- Y. Zhang, Y. Tao, Z. Yu, J. Lu, S. Y. Lim, J. Shao, "Structure and electrochemical properties of titanate perovskite with in situ exsolution as a ceramic electrode material", *J. Electroceram.*, **45** (2020) 29–38.

26. R.D. Shannon, "Revised effective ionic radii and systematic studies of interatomic distances in halides and chalcogenides", *Acta Cryst. A*, **32** (1976) 751–767.
27. J.I. Goldstein, D.E. Newbury, J.R. Michael, N.W.M. Ritchie, J.H.J. Scott, D.C. Joy, *Scanning Electron Microscopy and X-Ray Microanalysis*, Springer New York, NY, USA, 2017.
28. D.E. Newbury, N.W.M. Ritchie, "Performing elemental microanalysis with high accuracy and high precision by scanning electron microscopy/silicon drift detector energy-dispersive X-ray spectrometry (SEM/SDD-EDS)", *J. Mater. Sci.*, **50** [2] (2014) 493–518.
29. M.N. Rahaman, *Ceramic Processing and Sintering*, CRC Press, Boca Raton, USA, 2017.
30. G.L. Gurevich, A.K. Tagantsev, "Intrinsic dielectric loss in crystals: Low temperature", *Sov. Phys. JETP*, **64** (1986) 245–261.
31. G.L. Gurevich, A.K. Tagantsev, "Intrinsic dielectric loss in crystals", *Adv. Phys.*, **40** (1991) 719–767.
32. C.H. Shen, T.W. Shen, T.Y. Hsieh, K.C. Lan, S.H. Hsu, C.H. Wang, Y.T. Lin, W.F. Wu, Z.L. Tseng, "The enhanced thermal stability of $(\text{Mg}_{0.95}\text{Ni}_{0.05})_2\text{TiO}_4$ dielectric ceramics modified by a Multi-Phase Method", *Materials*, **16** (2023) 2997.